

A reduced orbital period for the supermassive black hole binary candidate in the quasar PG 1302-102?

D. J. D’Orazio^{1*}, Z. Haiman¹, P. Duffell², B. D. Farris^{1,3} and A. I. MacFadyen³

¹*Department of Astronomy, Columbia University, 550 West 120th Street, New York, NY 10027, USA*

²*Theoretical Astrophysics Center, Department of Astronomy, University of California, Berkeley, CA 94720, USA*

³*Center for Cosmology and Particle Physics, Physics Department, New York University, New York, NY 10003, USA*

Accepted 2015 June 30. Received 2015 June 26; in original form 2015 February 11

ABSTRACT

Graham et al. have detected a 5.2 yr periodic optical variability of the quasar PG 1302-102 at redshift $z = 0.3$, which they interpret as the redshifted orbital period $(1+z)t_{\text{bin}}$ of a putative supermassive black hole binary (SMBHB). Here, we consider the implications of a 3–8 times shorter orbital period, suggested by hydrodynamical simulations of circumbinary discs (CBDs) with nearly equal-mass SMBHBs ($q \equiv M_2/M_1 \gtrsim 0.3$). With the corresponding 2–4 times tighter binary separation, PG 1302 would be undergoing gravitational wave dominated inspiral, and serve as a proof that the BHs can be fuelled and produce bright emission even in this late stage of the merger. The expected fraction of binaries with the shorter t_{bin} , among bright quasars, would be reduced by one to two orders of magnitude, compared to the 5.2 yr period, in better agreement with the rarity of candidates reported by Graham et al. Finally, shorter periods would imply higher binary speeds, possibly imprinting periodicity on the light curves from relativistic beaming, as well as measurable relativistic effects on the Fe K α line. The CBD model predicts additional periodic variability on time-scales of t_{bin} and $\approx 0.5t_{\text{bin}}$, as well as periodic variation of broad line widths and offsets relative to the narrow lines, which are consistent with the observations. Future observations will be able to test these predictions and hence the binary+CBD hypothesis for PG 1302.

Key words: accretion, accretion discs – quasars: individual: PG 1302

1 INTRODUCTION

Graham et al. (2015, hereafter G15) recently reported strong optical variability of the quasar PG 1302-102, with an observed period of $t_{\text{obs}} = 5.2 \pm 0.2$ yr. G15 attribute the variability to the orbital motion of a super-massive black hole binary (SMBHB). Broad emission lines in the spectrum of PG 1302 imply a binary mass in the range $M = 10^{8.3-9.4} M_{\odot}$. Assuming that the binary’s orbital period t_{bin} equals the rest-frame optical variability period t_{opt} , G15 derive a fiducial binary separation $a \approx (0.0084 \pm 0.0003) \text{pc} \approx (276 \pm 9) R_{\text{S}}$ for $M = 10^{8.5} M_{\odot}$, where $R_{\text{S}} = 2GM/c^2$ is the Schwarzschild radius.

Hydrodynamical simulations of a binary BH embedded in a gaseous accretion disc predict that, depending on the binary mass ratio and the physical parameters of the disc, the strongest periodicity in the accretion rate on to the BHs may correspond to the motion of gas farther out in the disc, at a few times the binary separation, producing optical variability at several (~ 3 -8) times the binary orbital period. In this article, we discuss this expectation, and show that a reduced binary period, in the case of PG 1302, would have

several important implications. Follow up spectroscopy and photometric monitoring can determine the true binary period.

The rich variability structure of the mass accretion rates seen in simulations can be roughly divided into four distinct categories, based on the binary mass ratio $q \equiv M_2/M_1$. For $q \lesssim 0.05$, the disc is steady and the BH accretion rate displays no strong variability (D’Orazio et al. 2013; Farris et al. 2014; D’Orazio et al. in preparation). For $0.05 \lesssim q \lesssim 0.3$, the accretion rate varies periodically on the time-scale t_{bin} , with additional periodicity at $\approx 0.5t_{\text{bin}}$. Binaries with $0.3 \lesssim q \lesssim 0.8$ clear a lopsided central cavity in the disc, causing variability on three time-scales. The dominant period, $(3-8)t_{\text{bin}}$ is that of an over dense lump, orbiting at the ridge of the cavity, with additional periodicities at t_{bin} and $\approx 0.5t_{\text{bin}}$ (MacFadyen & Milosavljević 2008; Shi et al. 2012; Noble et al. 2012; Roedig et al. 2012; D’Orazio et al. 2013; Farris et al. 2014). The dominant period depends on the size of the cavity, and thus on disc parameters, such as temperature and viscosity. Finally, equal-mass ($q = 1$) binaries display variability at the longer lump period and at $\approx 0.5t_{\text{bin}}$.

Here, we consider the identification of the observed variability of PG 1302 with the long, cavity-wall period, and introduce the parameter $\chi \equiv t_{\text{opt}}/t_{\text{bin}}$, denoting the ratio, $3 \lesssim \chi \lesssim 8$, of the

* dorazio@astro.columbia.edu

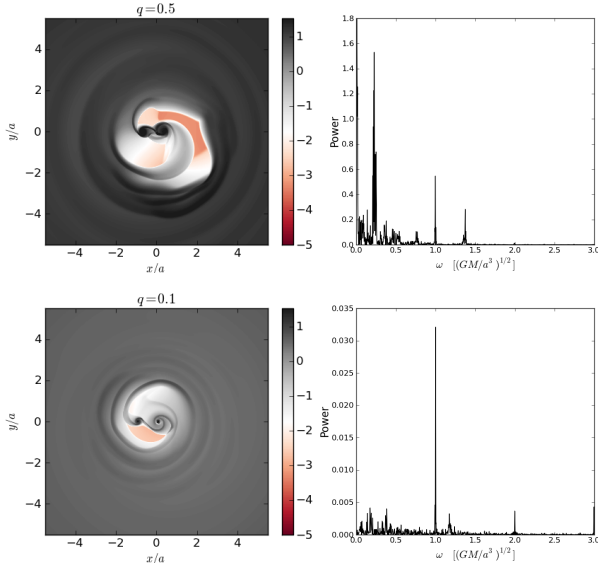


Figure 1. Results of 2D hydrodynamical simulations of a binary BH surrounded by a circumbinary accretion disc. The BHs clear out a central cavity and form their own minidisks. *Left-hand panels:* snapshots of the (logarithmic) surface-density of the gas discs, after reaching quasi-steady state, with mass ratios of $q = 0.5$ (top) and $q = 0.1$ (bottom). *Right-hand panels:* corresponding LSPs of the total accretion rate on to the secondary + primary BHs. The discs are locally isothermal with a Mach number of 10 and an alpha viscosity prescription ($\alpha = 0.1$).

observed rest-frame period and the true binary period. The binary separation is then

$$a \approx (94 \pm 3) R_S \left(\frac{\chi}{5} \right)^{-2/3} \left(\frac{M}{10^{8.5} M_\odot} \right)^{-2/3}, \quad (1)$$

or (0.0029 ± 0.0001) pc for the fiducial choices of χ and M .

In the rest of this article, we first (§2) explore several implications of a reduction in the binary’s orbital period, including the nature of PG 1302’s orbital decay and its ability to produce electromagnetic (EM) radiation (§2.1), the expected binary fraction of quasars (§2.2), and the detectability of gravitational waves (GWs) from PG 1302 by pulsar timing arrays (PTAs). We then (§3) propose possible observational tests of the underlying binary BH + circumbinary disc (CBD) model, including variations of broad line widths and centroids correlating with the optical variability (§3.1), additional periodic variability at the true t_{bin} caused by relativistic beaming (§3.2), signatures in the broad Fe K α lines (§3.2), and the existence of distinct secondary peaks in the periodogram (§3.3). We briefly summarize our main conclusions in §4.

2 IMPLICATIONS OF A SHORTER ORBITAL PERIOD

In order to demonstrate the possibility of a short orbital period for the PG 1302 binary, we have performed hydrodynamical simulations, following the set-up in our earlier work (Farris et al. 2014). The hydrodynamical equations are evolved for $\gtrsim 600$ binary orbits, using the two-dimensional code DISCO (Duffell & MacFadyen 2011), with the BHs moving on fixed circular orbits, surrounded by an isothermal (Mach number = 10) disc, obeying an α -viscosity prescription ($\alpha = 0.1$). The fluid motion around individual BHs is well resolved (with a log grid of 384 radial cells extending to $8a$ and a maximum of 512 azimuthal cells). The two runs discussed below differ only in their BH mass ratio ($q = 0.1$ and $q = 0.5$). A

wider range of simulations is needed in the future, to address possibilities such as eccentric (Roedig et al. 2012), tilted (Hayasaki et al. 2015), or retrograde (Nixon et al. 2011) binary orbits.

The results are illustrated in Fig 1. The left-hand panels show snapshots of the surface density, and the right-hand panels show Lomb Scargle periodograms (LSPs) of the total accretion rate measured in the two BH minidisks over 200 binary orbits. The top panels, for $q = 0.5$, show an over dense lump orbiting at the rim of the central cavity, resulting in strong periodicity at the orbital time $\approx 6t_{\text{bin}}$ of the lump. The periodogram shows weaker peaks at t_{bin} and at $\sim 0.6t_{\text{bin}}$. This three-time-scale behaviour, with the longest time-scale dominating, is observed for $0.3 \lesssim q \lesssim 0.8$. The location of the highest frequency peak is closer to $0.5t_{\text{bin}}$ near the low end of this range ($q \sim 0.3$), and also has a weak dependence on disc temperature and viscosity which must be quantified in future work. The bottom panels, for $q = 0.1$, show no orbiting lump and exhibit accretion rate periodicity only at t_{bin} and $0.5t_{\text{bin}}$. This behaviour is found in the range $0.05 \lesssim q \lesssim 0.3$.

Farris et al. (2014) have shown that for unequal-mass binaries, accretion occurs preferentially on to the secondary BH, with the ratio of accretion rates as skewed as $\dot{M}_2/\dot{M}_1 \approx 10 - 20$ in the range $0.02 \lesssim q \lesssim 0.1$. Over long time-scales, this would drive the binary to more equal masses, suggesting that mass ratios of $0.3 \lesssim q \lesssim 0.8$ may be common. Near-equal mass binaries are also preferred in cosmological models of the population of merging SMBHs (Volonteri et al. 2003).

Although there are large uncertainties in how accretion rate fluctuations turn into luminosity variations, we do expect the simulated accretion rate variations to lead to optical luminosity variations for PG 1302. The luminosity will follow local accretion rate fluctuations when the longer of the thermal or photon diffusion time-scale is much shorter than the accretion rate fluctuation time-scale ($\sim t_{\text{bin}}$). This is indeed the case where accretion modulations occur in our simulations, at the minidisc edges. Furthermore, optical emission is generated at the minidisks edges. We compute thin disc spectra for the CBD and minidisks. For the preferred mass range of PG 1302, near unity mass ratios, and the expected range of χ , the dominant optical component of the spectrum is generated by the low-energy tail of the blackbody emission from the outer edges of the minidisks, as well as (steady) emission from the inner regions of the CBD. Disc+binary simulations by Farris et al. (2015b), which self-consistently compute the local effective disc temperature not assuming a steady state, find results in agreement with our analytic reasoning: luminosity variations track the accretion-rate fluctuations, except at low frequencies where the quasi-steady CBD dominates.

The above lines of evidence motivate us to examine the possibility that the apparent 5.2 yr period in PG 1302 is the (redshifted) lump period, and assess the implications.

2.1 Binary-Disc Decoupling

A shorter orbital period would place the binary at a later stage of its orbital decay. A critical point during the orbital decay is the decoupling of the binary from the CBD, and it is important to know whether the binary is past this point. Here, we consider the decoupling radius for which the GW decay time-scale becomes shorter than the decay time-scale due to gaseous torques (so-called secondary-dominated Type II migration; Syer & Clarke 1995), outpacing the CBD. We use simple 1D models of the binary + disc system (Haiman et al. 2009, hereafter HKM09) to calculate the separation r_{GW} at which decoupling occurs for a circular binary with

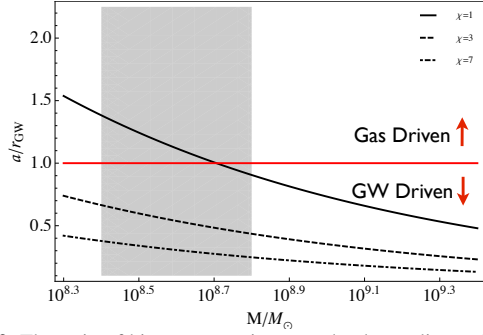


Figure 2. The ratio of binary separation a to the decoupling radius r_{GW} , for three different values of the ratio between the rest frame optical period and the true binary period, $\chi = t_{\text{opt}}/t_{\text{bin}}$. The shaded region marks the binary mass range inferred from the widths of broad lines measured by G15. For $\chi > 3$, the PG 1302 binary is past decoupling, for any choice of mass M .

mass ratio $q = 0.3$. We assume an α -viscosity $\nu = \alpha P_{\text{gas}}(\rho\Omega)^{-1}$, with gas pressure P_{gas} , density ρ , and disc angular velocity Ω . All other disc parameters are assumed to have the fiducial values given in HKM09. In Fig. 2, we plot the ratio a/r_{GW} as a function of the total binary mass M , with the binary separation from equation (1), for the range of masses in G15, and for three values of χ covering the range suggested by the hydrodynamical simulations.

Interpreting the observed variability in PG 1302 with t_{bin} , as may be justified for $q \lesssim 0.3$, it is unclear whether or not the binary has entered the GW dominated regime and decoupled from the disc. The binary would still be coupled to the disc for $M < 10^{8.7}M_{\odot}$ (the majority of the range inferred from the broad lines by G15), but GW-driven and decoupled if $M > 10^{8.7}M_{\odot}$. However, for the shorter binary periods $3 \lesssim \chi \lesssim 8$, justified for $0.3 \lesssim q \lesssim 0.8$, we find that the inferred smaller binary separation would place the binary well past decoupling. For $q > 0.3$ and $\alpha < 0.3$, the binary in PG 1302 is plunged even deeper into the GW-dominated regime.

Because the binary outpaces the disc, it has been argued that the post-decoupling BHs may be “starved” and thus dim (Milosavljević & Phinney 2005; Shapiro 2010; Tanaka & Menou 2010). Recent simulations (Noble et al. 2012; Farris et al. 2015a) show that high levels of accretion can persist well past the decoupling phase, delivering gas to the binary efficiently until much closer to coalescence. These simulations also exhibit the lopsided cavity which generates the χt_{bin} variability considered here. Identification of the variability in PG 1302 with the cavity wall lump period would constitute the (to our knowledge, first-ever) detection of an SMBHB which is undergoing GW dominated inspiral, yet producing bright emission, near the Eddington limit.¹

2.2 Binary Fraction among Quasars

A shorter binary orbit also reduces the expected number of detectable SMBHBs in quasars, because gas driven binaries are expected to spend less time at smaller separations. A simple estimate of the fraction of quasars that would harbour binaries with an orbital period t_{bin} can be obtained from the residence time $t_{\text{res}} = a/\dot{a}$ at each separation a , and the lifetime of bright ($L_Q/L_{\text{edd}} \gtrsim$

0.3) quasars, $t_Q \sim 10^8$ yr (Martini 2004). Assuming that a fraction f_{bin} of all quasars are triggered by coalescing SMBHBs (e.g Hopkins et al. 2007 and references therein), it follows that among bright quasars, the fraction with orbital period t_{bin} is $f_{\text{var}} = f_{\text{bin}}f_{\text{duty}}$, where $f_{\text{duty}} = t_{\text{res}}(t_{\text{bin}})/t_Q$ is the fraction of the bright quasar phase that a typical binary quasar spends at the orbital period t_{bin} .

We use the binary+disc models of HKM09 to predict the residence times of binaries. Prior to decoupling, t_{res} is determined by the binary’s interaction with the gas disc. For the masses and separations relevant for PG 1302, the disc would be radiation pressure dominated, yielding a relatively shallow power-law dependence $t_{\text{res}} \propto t_{\text{bin}}^{\beta}$ with $0.5 \lesssim \beta \lesssim 1.5$. These scalings depend on the poorly understood physical model of the disc and its coupling to the binary. Past decoupling, the residence time is precisely known, since it is determined by the strength of GWs. The dependence is much steeper, $t_{\text{res}} \propto t_{\text{bin}}^{8/3} \propto \chi^{-8/3}$. For reference, a binary with $M = 10^{8.5}M_{\odot}$ and $t_{\text{bin}} = 4\text{yr}$ would be in the disc-driven stage and would have $t_{\text{res}} \approx 10^6$ yr, yielding a large $f_{\text{duty}} \approx 10^{-2}$.

The expected f_{var} can be compared with the number of periodic candidates uncovered in CRTS (Drake et al. 2009; Djorgovski et al. 2011; Mahabal et al. 2011).² There are $\approx 114,000$ quasars in the CRTS sample with luminosity higher than PG 1302, ≈ 6 of which are SMBHB candidates with period $t_{\text{obs}} \lesssim 5\text{yr}$ (Graham, private communication), amounting to an observed fraction of $f_{\text{var}}^{\text{obs}} = 5 \times 10^{-5}$. Fig. 3 illustrates combinations of M , χ , and f_{bin} , for which we expect 1 (light grey regions) or 10 (dark grey) candidates in the CRTS quasar sample with periods ≤ 5.2 yr. Each shaded region is bounded by the assumed fraction of quasars related to SMBHBs at all, $f_{\text{bin}} = 0.01$ (left) to $f_{\text{bin}} = 1$ (right).

If the observed period of PG 1302 is assumed to be the binary orbital period ($\chi = 1$), then the rarity of the binary candidates in CRTS require $f_{\text{bin}} < 0.14$ (< 0.19) at $q = 0.3$ ($q = 1.0$), even at the most extreme mass of $M = 10^{9.4}M_{\odot}$. Taking the G15 fiducial mass of $M = 10^{8.5}M_{\odot}$, these fractions must be as low as $f_{\text{bin}} < 0.006$. These low values would be surprising, as a large fraction of quasars are commonly believed to be triggered by mergers. This association is based on various pieces of observational evidence, as well as on the success of merger-based quasar population models to reproduce many properties of the observed quasar population (e.g. Kauffmann & Haehnelt 2000). If, instead, the observed period of PG 1302 is due to the 3 – 8 times longer lump-periodicity, then the SMBHB fraction and the inferred binary mass of PG 1302-12 come into wider agreement with the expectation that $f_{\text{bin}} = O(1)$, e.g. allowing $f_{\text{bin}} \sim 0.3$ with $q = 0.3$ and $M = 10^{8.3}M_{\odot}$.

2.3 Detectability of GWs

A reduced orbital period increases the frequency and amplitude of GWs emitted by a binary, and it is interesting to ask whether PG 1302 may be detectable by present or future PTAs. The GW frequency, $f_{\text{GW}} = 2t_{\text{bin}}^{-1} \approx 61(\chi/5)$ nHz, places the binary in the range of PTA sensitivity (e.g. Hobbs et al. 2010). We calculate an SNR for the PG 1302 binary choosing optimistic binary parameters $M = 10^{9.4}M_{\odot}$, $q = 0.5$, and $t_{\text{bin}} = 1447\chi^{-1}$ d. The GW induced rms timing residual (for simplicity, adopting the sky and polarization averaged values) is $\delta t_{\text{GW}} =$

¹ Note that in the precessing binary model for OJ287 (Lehto & Valtonen 1996; Valtonen et al. 2008), the orbital period is 12.2 yr, the primary is very massive ($\sim 1.8 \times 10^{10}M_{\odot}$), but the secondary is light ($\sim 1.4 \times 10^8M_{\odot}$). The latter reduces the efficiency of GWs, but increases the impact of a gas disc; as a result, the OJ287 binary is gas-driven, well before decoupling.

² Since the expected $f_{\text{var}}(M, t_{\text{bin}})$ declines steeply with increasing M and decreasing t_{bin} , it is a good proxy for the fraction of quasars with period t_{bin} or less, and BH mass M or higher (or equivalently luminosity L or higher, further assuming a monotonic relation between L and M).

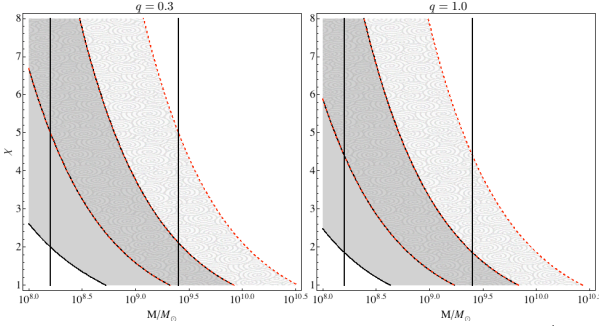


Figure 3. Combinations of total binary mass M and $\chi = t_{\text{opt}}/t_{\text{bin}}$ for which the predicted binary fraction of quasars matches 10 CRTS candidates with luminosity above that of PG 1302 (dark grey, bounded by solid curves), and for which it consists only of PG 1302 (light grey, bounded by red dashed curves). Vertical lines delineate the range of masses preferred by broad line widths. Each shaded region is bounded by the fraction f_{bin} of quasars which are triggered by a binary. In each case, the lines correspond to $f_{\text{bin}} = 0.01, 0.1, 1$ (left to right).

$\sqrt{8/15}h/(2\pi f_{\text{GW}})\sqrt{f_{\text{GW}}T} \approx 2.6(\chi/5)^{1/6}\sqrt{T_{\text{yr}}}$ ns for a one year observation time T_{yr} ; for $f_{\text{GW}} \gtrsim 10$ nHz, the timing residual noise is nearly constant in frequency. Using noise curves of currently operating PTAs, the SNR for GW detection of the PG 1302 binary is $\sim 0.005(\chi/5)^{1/6}\sqrt{T_{\text{yr}}}$ for NANOGrav (fig. 12 in Arzoumanian et al. 2014) or $\sim 0.011(\chi/5)^{1/6}\sqrt{T_{\text{yr}}}$ for the PPTA (black curve in fig. 9 of Zhu et al. 2014). The reduced binary period increases the SNR, but this increase is unfortunately modest. Future detectors, such as the international pulsar timing array (IPTA; Manchester & IPTA 2013) as well as inclusion of the square kilometre array (SKA; Dewdney et al. 2009) in the PTA telescope networks will improve the SNR by about an order of magnitude, but PG 1302 will remain a factor of ~ 10 below detection.

3 TESTING THE BINARY BH SCENARIO FOR PG 1302

3.1 Broad Line Variability and Asymmetry

Jackson et al. (1992) report a $\sim (150 \pm 50)\text{km s}^{-1}$ offset between the broad and narrow line components of PG1302’s $\text{H}\beta$ emission line. This is much smaller than the secondary BH’s orbital speed, $v_2 = 14,500(1.5/[1+q])(M/10^{8.5}M_{\odot})^{1/3}(\chi/5)^{1/3}\text{km s}^{-1}$, or the width of the broad lines. Such larger offsets have been predicted for binary SMBHs, assuming that the broad line region (BLR) originates from gas bound to one component of a binary SMBH and thus shares its overall orbital motion (e.g Tsalmantza et al. 2011). Here we argue that the smaller offset for PG1302 can also be attributed to a binary SMBH, assuming that the BLR is located farther out, in the circumbinary gas. Using simple toy models, we show that the lopsided geometry of the CBD gas (Fig. 1) could generate the small observed offset but large width of PG 1302’s broad $\text{H}\beta$ line. The models below are meant to be mere illustrations; a self-consistent description of the BLR is left to future work.

The idea is that the large width of a line can reflect the orbital speed of gas in the CBD (over a range of annuli), whereas the offset of the line centroid is caused only by departures from axisymmetry and can be much smaller. (In a strictly axisymmetric BLR, the blue- and redshifts from gas on opposing sides of the binary would be the same and leave no net offset). To illustrate this, we compute the line offset V_0 as the emission-weighted line-of-sight (l.o.s.) velocity,

$$V_0 = \frac{\int_0^{2\pi} \int_{\mathcal{R}} \rho^n (v_{\phi}/r)^m v_{\text{los}} r dr d\phi}{\int_0^{2\pi} \int_{\mathcal{R}} \rho^n (v_{\phi}/r)^m r dr d\phi} \quad (2)$$

and the width Γ as the weighted rms l.o.s. velocity

$$\left(\frac{\Gamma}{2\sqrt{2\ln 2}}\right)^2 = \frac{\int_0^{2\pi} \int_{\mathcal{R}} \rho^n (v_{\phi}/r)^m (v_{\text{los}} - V_0)^2 r dr d\phi}{\int_0^{2\pi} \int_{\mathcal{R}} \rho^n (v_{\phi}/r)^m r dr d\phi} \quad (3)$$

over a surface patch \mathcal{R} in a $q = 0.5$ simulation (see Fig. 1).

In order to select the scaling indices n and m , and to identify a patch \mathcal{R} corresponding to the BLR, we first consider a steady thin disc model for the CBD (as in §2), and assume that the CBD is illuminated by a central ionizing source (i.e. the minidisks). For PG1302’s parameters, the inner region of the CBD would have density $n \sim 10^{12-13}\text{cm}^{-3}$ and would be highly opaque to ionizing radiation. In this case, recombinations in a volume corresponding to a very thin ($\Delta R \ll R$) inner annulus of the CBD would balance the central ionizing photon rate. In particular, the disc would absorb the covering fraction $2\pi RH/(4\pi R^2) = 0.05H/(0.1R)$ of the central luminosity. PG 1302’s bolometric luminosity is $\sim 6 \times 10^{46}\text{erg s}^{-1}$; assuming that $\gtrsim 1/3$ rd of this is emitted in the UV, $\gtrsim 5\%$ of which is absorbed by the CBD (i.e. $H/R \gtrsim 0.1$), this would be sufficient to provide the total power $\sim 10^{45}\text{erg s}^{-1}$ measured in the broad lines (Wang et al. 2003). The line emission from each patch of the CBD depends only upon the number of ionizing photons incident on the CBD in that direction, i.e. proportional to the scale height H of the inner wall of the CBD. For an adiabatic scale height, assuming vertical disc hydrostatic equilibrium, $n = 1/3$ and $m = -1$. To be specific, \mathcal{R} is chosen by excising the binary plus minidisks, and imposing a surface density range $\Sigma/\Sigma_0 = (0.01, 0.5)$. While somewhat ad hoc, we find that this Σ range accurately picks out the streams edges inside the cavity, and the thin inner edges of the CBD.

Although a standard Shakura-Sunyaev CBD is optically thick outside of the inner cavity, we also consider, for generality, an alternative scenario, where the BLR emission is produced by an optically thin medium, but still resembling the lopsided geometry in our simulations. In this case, line emission would scale with the recombination rate, with $n = 2$ and $m = 0$ in equations. 3. We adopt the region \mathcal{R} to be an annulus with inner and outer radii $(2a, 6a)$, chosen to encompass the inner CBD.

We use the simulated surface density Σ , azimuthal velocity v_{ϕ} and the inferred isothermal scale height of the disc $H = rc_s/v_{\phi}$ (assuming vertical hydrostatic equilibrium), to compute the volume density $\rho = \Sigma/H$ and l.o.s. velocity $v_{\text{los}} = v_{\phi} \cos \phi$. All l.o.s. velocities are multiplied by an additional factor of $\sin i$, where i is the CBD inclination angle, measured from face-on. We calculate V_0 and Γ 10 times per orbit for 20 orbits. Fig. 4 displays the variations of V_0 and Γ with time for the optically thin case. The line centroid varies with mean and range

$$\begin{aligned} V_0^{\text{thin}} &= (2 \pm 167) \left[\frac{\sin i}{\sin(14.1^\circ)} \right] \frac{\text{km}}{\text{s}} \left(\frac{M}{10^{8.5}M_{\odot}} \right)^{\frac{1}{2}} \left(\frac{a}{94R_S} \right)^{-\frac{1}{2}}, \\ V_0^{\text{thk}} &= (-5 \pm 285) \left[\frac{\sin i}{\sin(11.4^\circ)} \right] \frac{\text{km}}{\text{s}} \left(\frac{M}{10^{8.5}M_{\odot}} \right)^{\frac{1}{2}} \left(\frac{a}{94R_S} \right)^{-\frac{1}{2}}, \end{aligned}$$

while the line full width at half-maximum (FWHM) fluctuates periodically on the lump’s orbital time,

$$\begin{aligned} \Gamma^{\text{thin}} &= (4450 \pm 615) \left[\frac{\sin i}{\sin(14.1^\circ)} \right] \frac{\text{km}}{\text{s}} \left(\frac{M}{10^{8.5}M_{\odot}} \right)^{\frac{1}{2}} \left(\frac{a}{94R_S} \right)^{-\frac{1}{2}}, \\ \Gamma^{\text{thk}} &= (4450 \pm 636) \left[\frac{\sin i}{\sin(11.4^\circ)} \right] \frac{\text{km}}{\text{s}} \left(\frac{M}{10^{8.5}M_{\odot}} \right)^{\frac{1}{2}} \left(\frac{a}{94R_S} \right)^{-\frac{1}{2}}. \end{aligned}$$

The fiducial inclination angles above are chosen to match the observed $\text{H}\beta$ FWHM.

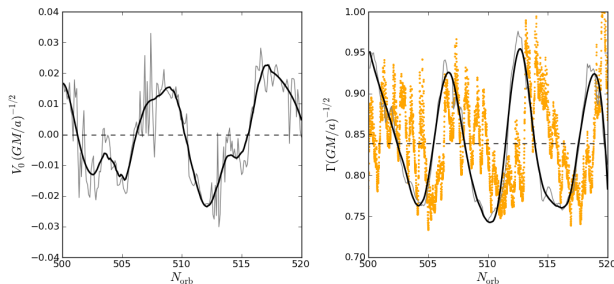


Figure 4. Predicted variations of the centroid V_0 (left) and FWHM Γ (right) of an emission line emanating from the inner CBD. The total accretion rate on to both black holes is over plotted in the right-hand panel in arbitrary units (orange). Dark black lines are smoothed versions of the light grey simulation data.

We find that both models of a CBD BLR predict a line offset consistent with that observed in Jackson et al. (1992) and which require a CBD inclination angle that also predicts consistent line widths. Additionally, we find that Γ varies by up to ~ 14 per cent of the mean in each case. It is important to emphasize that in the optically thick case, these results arise from the non-axisymmetric velocities in the gas that trace the lopsided inner wall of the CBD, whereas in the optically thin case, they are driven by the lopsided density distribution.

Since fluctuations in the latter case arise from the lump’s varying position along the cavity wall, they correlate with long-term variations in the BH accretion rate. In the right-hand panel of Fig. 4, we plot the accretion rate on to the BHs, together with the Γ variations of the optically thin case. The phase lag between line-width maximum and accretion maximum derives from the time between lump passage near the BHs, and the lump-enhanced accretion in the minidisks. The phase difference is therefore independent of the observer’s viewing angle. This is not true for the amplitude and shape of the FWHM variations, and the relative phase of $V_0(t)$, which depend on viewing angle. For the optically thick case, the FWHM variations are similar, except that they have a $\sim 20\%$ higher mean, and are \sim half a cycle out of phase with the accretion rate modulation. The phase difference arises because the optically thick model tracks the low density gas at the cavity and stream edges instead of the high density lump. The centroid variations are also similar in the optically thick case but have a few times higher mean and deviation because they track the eccentric cavity shape rather than a symmetric annulus.

The line characteristics which we calculate here are dependent on the existence and magnitude of the orbiting cavity wall overdensity (requiring $3 \lesssim \chi \lesssim 8$). As long as the binary has mass ratio such that a cavity wall lump is generated, our BLR calculation is largely unchanged. In addition to mass ratio, disc viscosity and temperature affect the lump size and thus the magnitude of broad line variations. The line shape also depends on the broad line emission model. Hence, a full study of CBD broad lines, which examines more sophisticated recombination models and a range of disc parameters, binary mass ratios and viewing angles, is warranted in a future study. Parameter dependences aside, observation of line variability, matched to luminosity variability, would provide evidence for the CBD model and the origin of the BLR as well as identification of the CBD cavity wall period.

3.2 Relativistic Effects

Beaming. D’Orazio et al. (2015) have shown that if PG1302 con-

sists of a massive ($M \gtrsim 10^9 M_\odot$) but unequal-mass ($0.03 \lesssim M_2/M_1 \lesssim 0.1$) SMBH binary, seen within $\lesssim 30^\circ$ of edge-on, then the entire 0.14 mag variability of PG 1302 can be explained by relativistic Doppler boost. In the hydrodynamical explanation proposed here, where the 5.2-yr modulation arises from variations in the accretion rate, relativistic boost would also inevitably imprint additional sinusoidal modulations at the true (shorter) binary period. The effect would be enhanced, because the secondary’s velocity is higher by a factor of $\chi^{1/3}$, potentially causing a detectable second peak in the periodogram at $5.2\chi^{-1}$ yr. Requiring consistency with § 3.1, we use the maximum binary mass and minimum mass ratio ($q = 0.03$) to put an upper limit on the secondary’s l.o.s. velocity v_{los} . The relativistic beaming factor is $[\Gamma(1 - v_{\text{los}}/c)]^{\alpha-3}$, where Γ is the Lorentz factor. D’Orazio et al. (2015) have estimated the spectral index $\alpha = 1.1$ from an average over the continuum in the V band. We find that the corresponding maximum velocity imprints a 0.07 mag amplitude modulation on PG 1302’s light curve. PG 1302’s periodogram does not show a significant secondary peak with sub-5.2 yr periods, but noise modelling suggests that such second peaks would be detectable only at amplitudes of $\gtrsim 0.07\text{mag}$, \sim half of the 5.2-yr modulation (Charisi et al. 2015, see the next section).

Iron K α lines. Because the binary separation can be reduced below $\lesssim 100R_S$, FeK α lines generated at such small separations can have characteristic binary-related features, such as ‘missing wings’ (due to the central cavity), or ‘see-saw oscillations’ of the red and blue wings (due to Doppler-shifting of the emission from minidisks; McKernan et al. 2013). These may be detectable with the upcoming Astro-H mission (Takahashi et al. 2014).

3.3 Orbital time-scale Variability

The binary+CBD model discussed above generically predicts multiple periodic variations. If the observed period of PG 1302 is the true binary period, then its periodogram could contain lower frequency, higher-amplitude, and also higher frequency, lower amplitude peaks. These could be revealed in future data, combined with more sophisticated search algorithms for periodicity (e.g. VanderPlas & Ivezić 2015 and references therein). It will be helpful in such a search that two of the periodicities occur at t_{bin} and $\approx 0.5t_{\text{bin}}$, i.e. with a characteristic 1:2 ratio in frequency. These are expected to be the only two peaks present for $0.05 \lesssim q \lesssim 0.3$. The variability at t_{bin} can disappear entirely, but this happens only in the limit of $q \rightarrow 1$ (presumably rarely realized in nature). Thus the detection of a secondary peaks, and the characterization of the full variability structure, can help confirm the binary nature of PG 1302, and constrain its parameters. Charisi et al. (2015) searched PG 1302’s available photometric data for the existence of additional peaks at frequencies above or below the strongest and unambiguous 5.2 yr period. No significant peaks were detected, and an upper limit of $\delta m \gtrsim 0.07 - 0.14$ mag (depending on frequency) was derived for the amplitude of additional modulations.

4 CONCLUSIONS

For binaries with mass ratio in the range $0.3 \lesssim q \lesssim 0.8$, hydrodynamical simulations of CBDs predict dominant luminosity variations at 3–8 times the binary orbital period, due to a dense lump in the CBD (Fig. 1). If the periodic variability observed in quasar PG 1302 is identified with this lump period, rather than the orbital period of a putative SMBHB, a two to four times smaller binary separation is inferred. This would place the PG 1302 binary securely in

the GW-driven regime, making it the first EM detection of such a system, and proving that gas can follow the binary past decoupling. This is encouraging for the possibility of locating EM counterparts of GW sources. Because binaries spend less time at smaller separations, a shorter t_{bin} is in better agreement with the small number of SMBHB candidates reported by G15. The higher orbital velocity of the binary increases the effects of relativistic beaming, causing optical variability at the orbital period, and also on inferred broad line widths.

The binary+CBD model can be tested as it predicts variability at multiple, well-defined frequencies which depend on binary mass ratio and disc parameters. Since a recent search (Charisi et al. 2015) did not reveal secondary variability in the optical light curve of PG 1302, follow up observations are required. Finally, associating the BLR with the inner annuli of a lumpy CBD, we find that the FWHM of the lines can vary at the period of the continuum variability by ± 14 per cent; we also predict a much smaller shift of the broad line centroids. These predictions are consistent with existing observations of the width and offset of the $H\beta$ broad line. Follow-up spectra, sampling PG 1302’s apparent 5.2 yr period, could test this interpretation of the BLR and aid in identifying the nature of PG 1302’s variability.

ACKNOWLEDGEMENTS

Resources supporting this work were provided by the NASA High-End Computing (HEC) Programme through the NASA Advanced Supercomputing (NAS) Division at Ames Research Center and by the High Performance Computing resources at Columbia University. The authors thank Maria Charisi, Imre Bartos, Adrian Price-Whelan, Jules Halpern, and Roman Rafikov for useful discussions. We also thank Matthew Graham and George Djorgovski for useful information on PG 1302, as well as for providing the light curve in electronic form. We also thank the anonymous referee for comments that helped to improve this Letter. We acknowledge support from a National Science Foundation Graduate Research Fellowship under Grant no. DGE1144155 (DJD) and NASA grant NNX11AE05G (ZH and AMF).

REFERENCES

- Arzoumanian Z., et al., 2014, *ApJ*, 794, 141
 Charisi M., Bartos I., Haiman Z., Price-Whelan A. M., Márka S., 2015, *ArXiv e-prints*
 Dwdney P. E., et al., 2009, *IEEE Proceedings*, 97, 1482
 Djorgovski S. G., et al., 2011, *ArXiv e-prints*
 D’Orazio D. J., Haiman Z., MacFadyen A., 2013, *MNRAS*, 436, 2997
 D’Orazio D. J., Haiman Z., Schiminovich D., 2015, *Nature*, in press
 Drake A. J., et al., 2009, *ApJ*, 696, 870
 Duffell P. C., MacFadyen A. I., 2011, *ApJS*, 197, 15
 Farris B. D., Duffell P., MacFadyen A. I., Haiman Z., 2014, *ApJ*, 783, 134
 Farris B. D., Duffell P., MacFadyen A. I., Haiman Z., 2015a, *MNRAS*, 447, L80
 Farris B. D., Duffell P., MacFadyen A. I., Haiman Z., 2015b, *MNRAS*, 446, L36
 Graham M. J., et al., 2015, *Nature*, 518, 74
 Haiman Z., Kocsis B., Menou K., 2009, *ApJ*, 700, 1952
 Hayasaki K., Sohn B. W., Okazaki A. T., Jung T., Zhao G., Naito T., 2015, *JCAP*, 7, 5
 Hobbs G., et al., 2010, *Classical and Quantum Gravity*, 27, 084013
 Hopkins P. F., Bundy K., Hernquist L., Ellis R. S., 2007, *ApJ*, 659, 976
 Jackson N., et al., 1992, *A&A*, 262, 17
 Kauffmann G., Haehnelt M., 2000, *MNRAS*, 311, 576
 Lehto H. J., Valtonen M. J., 1996, *ApJ*, 460, 207
 MacFadyen A. I., Milosavljević M., 2008, *ApJ*, 672, 83
 Mahabal A. A., et al., 2011, *Bulletin of the Astronomical Society of India*, 39, 387
 Manchester R. N., IPTA 2013, *Class. Quantum Grav.*, 30, 224010
 Martini P., 2004, *Coevolution of Black Holes and Galaxies*, p. 169
 McKernan B., Ford K. E. S., Kocsis B., Haiman Z., 2013, *MNRAS*, 432, 1468
 Milosavljević M., Phinney E. S., 2005, *ApJ*, 622, L93
 Nixon C. J., Cossins P. J., King A. R., Pringle J. E., 2011, *MNRAS*, 412, 1591
 Noble S. C., Mundim B. C., Nakano H., Krolik J. H., Campanelli M., Zlochower Y., Yunes N., 2012, *ApJ*, 755, 51
 Roedig C., Sesana A., Dotti M., Cuadra J., Amaro-Seoane P., Haardt F., 2012, *A&A*, 545, A127
 Shapiro S. L., 2010, *Physical Review D*, 81, 24019
 Shi J.-M., Krolik J. H., Lubow S. H., Hawley J. F., 2012, *ApJ*, 749, 118
 Syer D., Clarke C. J., 1995, *MNRAS*, 277, 758
 Takahashi T., Mitsuda K., Kelley R., Fabian A., Mushotzky R., Ohashi T., Petre R., on behalf of the ASTRO-H Science Working Group 2014, *ArXiv e-prints*
 Tanaka T., Menou K., 2010, *ApJ*, 714, 404
 Tsalmantza P., Decarli R., Dotti M., Hogg D. W., 2011, *ApJ*, 738, 20
 Valtonen M. J., et al., 2008, *Nature*, 452, 851
 VanderPlas J. T., Ivezić Z., 2015, *ApJ*, submitted; e-print [arXiv:1502.01344](https://arxiv.org/abs/1502.01344)
 Volonteri M., Haardt F., Madau P., 2003, *ApJ*, 582, 559
 Wang J.-M., Ho L. C., Staubert R., 2003, *A&A*, 409, 887
 Zhu X.-J., et al., 2014, *MNRAS*, 444, 3709